WRF-LES Simulation of Wind Flow over Rough Urban Surface during Typhoon Lan (2017)

Keigo Nakajima[1], Hidenori Kawai[2], Masaharu Kawaguchi[3], Tetsuro Tamura[4], Koji Kondo[5], Yoshiaki Itoh[6] and Kenji Takagi[7]

[1] Kajima Corporation
2-19-1 Tobitakyu, Chofu-shi, Tokyo, Japan
nakakeig@kajima.com

[2] Ochanomizu University
2-1-1 Otsuka, Bunkyo-ku, Tokyo, Japan
kawai.hidenori@ocha.ac.jp

[3] Tokyo Institute of Technology
2-12-1 Ookayama, Meguro-ku, Tokyo, Japan
kawaguchi.m.ag@m.titech.ac.jp

[4] Tokyo Institute of Technology
2-12-1 Ookayama, Meguro-ku, Tokyo, Japan
tamura.t.ab@m.titech.ac.jp

[5] Kajima Corporation
2-19-1 Tobitakyu, Chofu-shi, Tokyo, Japan
kondokoj@kajima.com

[6] Kajima Corporation
2-19-1 Tobitakyu, Chofu-shi, Tokyo, Japan
itohyoshiaki@kajima.com

[7] Kajima Corporation
2-19-1 Tobitakyu, Chofu-shi, Tokyo, Japan
takagik@kajima.com

Key words: WRF-LES, Typhoon, Urban Area, Mean Wind Speed, Wind Speed Fluctuation

Abstract. *In this study, we investigated the influence of ground surface boundary conditions of the meteorological model on the accuracy in predicting the mean wind speed and wind speed fluctuation in the urban area. Two types of ground surface boundary conditions (Cases 1 and 2) were created. In Case 1, the roughness length for the urban area was set to 0.5 m uniformly, whereas in Case 2, the spatial distribution of roughness length for the urban area was set based on the urban geometry. We performed the wind flow simulation in the central part of Tokyo during Typhoon Lan (2017) by using WRF-LES with the created ground surface boundary conditions. By setting the roughness length based on the urban geometry, the accuracy in predicting the mean wind speed was improved significantly. However, in both cases, WRF-LES*

underestimated the turbulence intensity, especially near the ground surface.

1 INTRODUCTION

In LES (Large-Eddy Simulation) to evaluate wind load acting on buildings, the turbulent boundary layer flow is typically set as inflow data. However, the effect of meteorological disturbances due to large-scale flow structures [1, 2, 3] cannot be considered sufficiently in this method. Attempts have recently been made to generate LES inflow data that include the effect of meteorological disturbances by using meteorological models [4] and further advancement of wind load evaluation using LES is expected. In the previous study, we indicated that the meteorological model overestimated the mean wind speed in an urban area because of the underestimation of ground surface friction [5]. The prediction accuracy of meteorological models in urban areas needs to be improved to generate LES inflow data that include the effect of meteorological disturbances adequately.

In this study, we investigated the influence of ground surface boundary conditions of the meteorological model on the accuracy in predicting the mean wind speed and wind speed fluctuation in an urban area. Two types of ground surface boundary conditions were created. In one case, the roughness length for the urban area was set to 0.5 m uniformly (default setting), whereas in the other case, the spatial distribution of roughness length for the urban area was set based on the urban geometry [6, 7, 8]. We performed wind flow simulations in the central part of Tokyo during Typhoon Lan (2017) using the meteorological model with the created ground surface boundary conditions. The simulation results were compared with observation data at multiple locations.

2 METHOD

WRF (Weather Research and Forecasting model) [9] and WRF-LES (LES mode of WRF) [9] were used as the meteorological models. Figure 1 shows the analysis domains and Table 1 lists the analysis conditions of WRF and WRF-LES. The analysis domains consisted of Domains 1 – 5. WRF was applied to the simulation in Domains 1 – 3 and WRF-LES was applied to the simulation in Domains 4 – 5. The sizes of Domains 1 – 3 (WRF) were 1377 km × 1377 km, 756 km × 756 km and 300 km × 300 km, and their horizontal grid resolutions were 9 km, 3 km and 1 km, respectively. The sizes of Domains 4 – 5 (WRF-LES) were 40 km × 40 km and 20 km × 20 km, and their horizontal grid resolutions were 250 m and 50 m, respectively. The planetary boundary layer scheme of WRF was YSU scheme [10] and the SGS model of WRF-LES was 1.5 order TKE closure model [11]. Other physical models of WRF and WRF-LES are presented in Table 1.

The target of the simulation was Typhoon Lan (2017). The final analysis data set (FNL) (1 deg resolution) of NCEP (National Centers for Environmental Prediction) was used for the initial and boundary conditions of WRF. However, the real-time global sea surface temperature data set (RTGSST) (0.25 deg resolution) of NCEP was used for the sea surface temperature. The connection between WRF and WRF-LES was conducted by one-way nesting, wherein the initial and boundary conditions of WRF-LES (Domain 4) were created from the results of WRF (Domain 3). The WRF simulation in Domains 1 – 3 and WRF-LES simulation in Domains 4 – 5 were conducted by two-way nesting, wherein the data were exchanged between each domain.
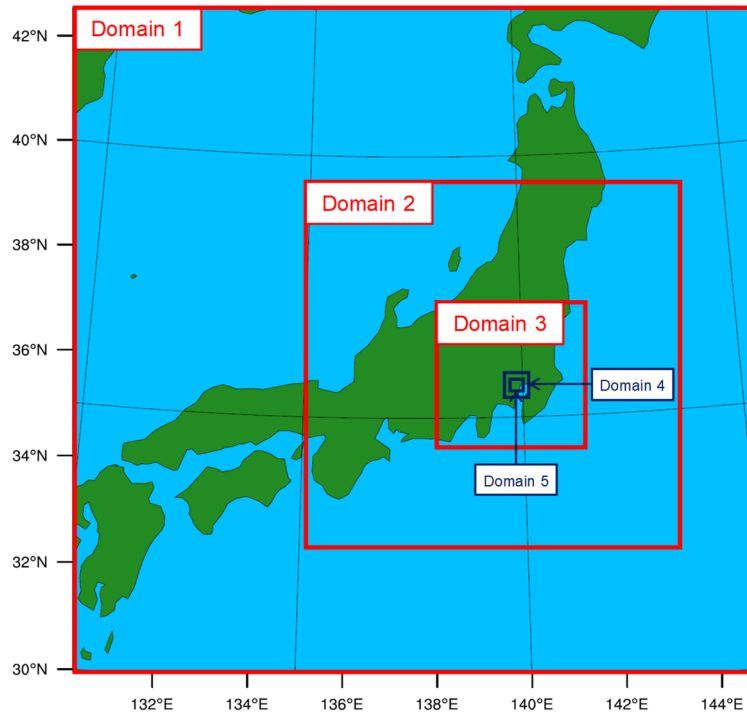
Figure 1: Analysis domains of WRF and WRF-LES (Domains 1 – 3: WRF, Domains 4 – 5: WRF-LES)

Table 1: Analysis conditions of WRF and WRF-LES

	Domains 1 – 3 (WRF)	Domains 4 – 5 (WRF-LES)
Analysis domain	1377 km × 1377 km (Domain 1) 756 km × 756 km (Domain 2) 300 km × 300 km (Domain 3)	40 km × 40 km (Domain 4) 20 km × 20 km (Domain 5)
Time resolution	9 s (Domain 1) 3 s (Domain 2) 1 s (Domain 3)	0.25 s (Domain 4) 0.05 s (Domain 5)
Horizontal grid resolution	9 km (Domain 1) 3 km (Domain 2) 1 km (Domain 3)	250 m (Domain 4) 50 m (Domain 5)
Number of vertical layer	75 layers (Minimum layer thickness: 60 m)	150 layers (Minimum layer thickness: 30 m)
Planetary boundary layer scheme	YSU scheme	
SGS model		1.5 order TKE closure model
Land surface model	Unified Noah land surface model	
Surface layer scheme	Revised MM5 Monin-Obukhov scheme	
Microphysics scheme	WSM 6-class graupel scheme	
Cumulus convective parameterization scheme	Kain-Fritsch scheme (Domain 1)	
Long wave radiation scheme	RRTMG scheme	
Short wave radiation scheme		

The WRF simulation was performed from 12:00 UTC on October 22 to 00:00 UTC on October 23, 2017 and WRF-LES simulation was performed from 17:30 UTC to 21:30 UTC on October 22, 2017. Hereafter, time is expressed in UTC (Coordinated Universal Time).

The data set of USGS (United States Geological Survey) (30 s resolution) was used for the land use category in Domains 1 – 3 (WRF) and the data set of GSI (Geospatial Information Authority of Japan) (10 m resolution) was used for the land use category in Domains 4 – 5 (WRF-LES). Table 2 shows the roughness length for each land use category. In this study, two types of ground surface boundary conditions (Cases 1 and 2) were created. In Case 1, the roughness length for "Urban and Built-up Land" was set to 0.5 m uniformly (default setting), whereas in Case 2, the spatial distribution of roughness length for "Urban and Built-up Land" was set based on the urban geometry [6, 7, 8]. Figure 2 shows the spatial distribution of the roughness length in Domain 4 (WRF-LES). The blue areas in Figure 2 are "Water Bodies" and the black areas in Figure 2 are "Dryland Cropland and Pasture", "Irrigated Cropland and Pasture", "Grassland" and "Mixed Forest". In Case 2, the roughness length in the central part of Tokyo was much larger than 0.5 m and ranged from approximately 4 to 20 m.

Table 2: Roughness length for each land use category

Land use category	Roughness length
Urban and Built-up Land	Case 1: 0.5 m (see Figure 2a) Case 2: see Figure 2b
Dryland Cropland and Pasture	0.15 m
Irrigated Cropland and Pasture	0.1 m
Grassland	0.12 m
Mixed Forest	0.5 m
Water Bodies	0.0001 m

a) Case 1   b) Case 2
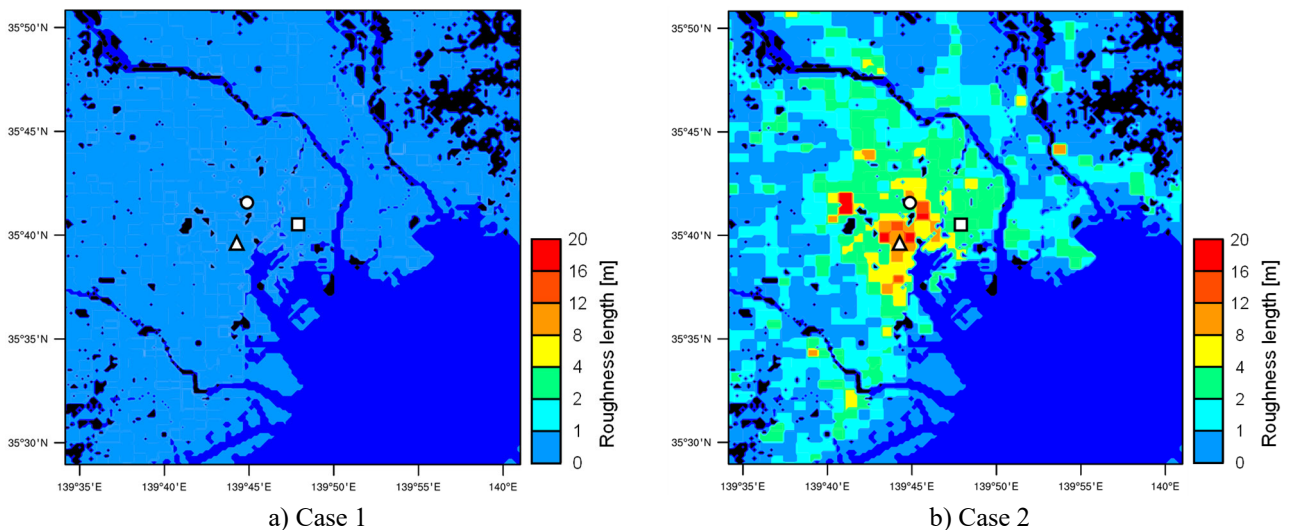
Figure 2: Spatial distribution of roughness length in Domain 4
(○: Location A (Tokyo District Meteorological Observatory), △: Location B (Tokyo Tower) and □: Location C (Kiba))

3 RESULT

3.1 Track and central pressure of the typhoon (WRF)

Figure 3 shows the track and central pressure of the typhoon. The plot in Figure 3 shows the center of the typhoon every 1 h in WRF and every 3 h in the best track. In WRF, the landfalling time of the typhoon roughly agreed with that in the best track, but the moving speed of the typhoon after the landfall was slower than that in the best track. When the typhoon came closest to the central part of Tokyo, the track of the typhoon in WRF shifted to the west compared with that in the best track. In WRF, the central pressure of the typhoon was higher than that in the best track. However, after landfall, the central pressure of the typhoon in WRF approached that in the best track.

The results of the WRF simulation in Domains 1 – 3 were used to create the initial and boundary conditions of the WRF-LES simulation in Domains 4 – 5. From next section, the results of the WRF-LES simulation are presented.

a) Track of the typhoon   b) Central pressure of the typhoon
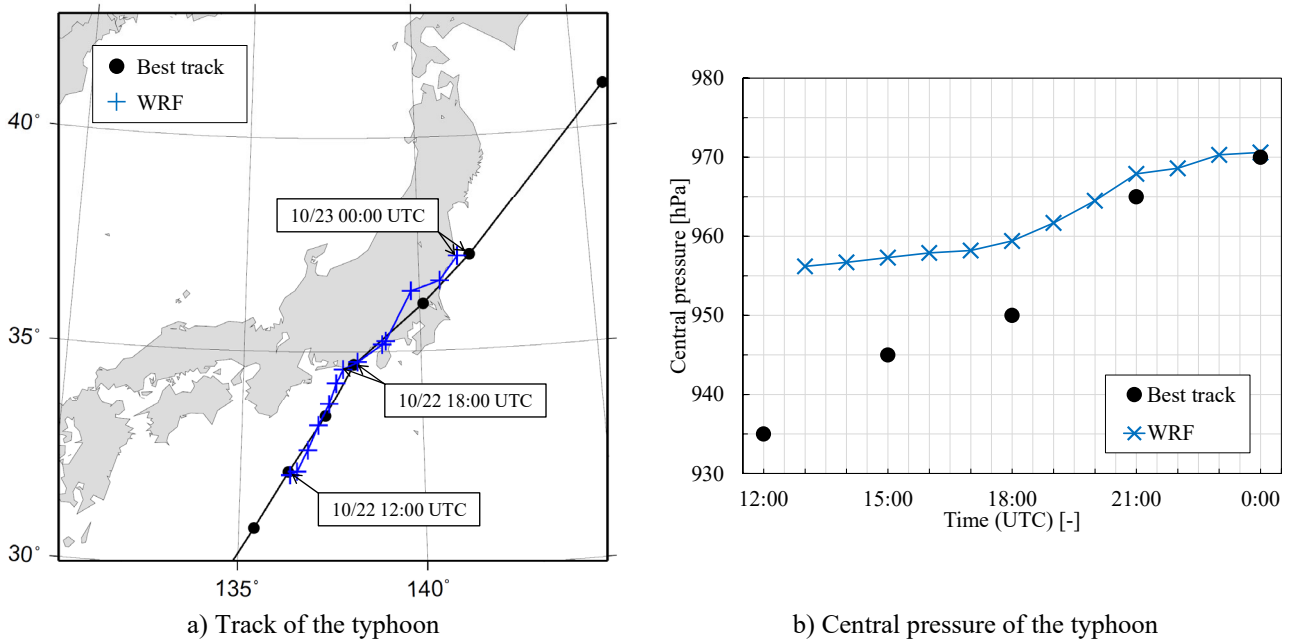
Figure 3: Track and central pressure of the typhoon

3.2 Mean wind speed (WRF-LES)

Figure 4 shows the time variation of the 10-min mean wind speed and wind direction at Location A (Tokyo District Meteorological Observatory, see Figure 2). Although the 10-min mean wind direction from 18:30 to 20:30 in WRF-LES agreed well with that in the observation, the 10-min mean wind direction from 17:30 to 18:30 and from 20:30 to 21:30 in WRF-LES was largely different from that in the observation. This was likely caused by the error of the track of the typhoon in the WRF simulation (Domains 1 – 3). At Location A, the 10-min mean wind speed in Case 2, wherein the roughness length was set based on the urban geometry, was smaller than that in Case 1. The maximum value of the 10-min mean wind speed in Case 2

agreed well with that in the observation.

Figure 5 shows the vertical profile of the mean wind speed from 18:30 to 19:00 at Locations A, B (Tokyo Tower, see Figure 2) and C (Kiba, see Figure 2). The mean wind speed was normalized by the value at an altitude of 250 m. The observation data at Locations B and C [12] are shown in Figure 5. The mean wind direction from 18:30 to 19:00 at Locations A, B and C at an altitude of 250 m was south-southeast, wherein the wind flowed from the coastal area to the urban area. The power law exponent calculated from the vertical gradient of the mean wind speed at altitudes lower than 250 m was 0.40 for Case 1 and 0.57 for Case 2 at Location A, 0.55 for the observation, 0.38 for Case 1 and 0.55 for Case 2 at Location B, 0.69 for the observation, 0.35 for Case 1 and 0.46 for Case 2 at Location C. In Case 2, the vertical gradient of the mean wind speed was larger than that in Case 1 at Locations A, B and C. At Location B, the vertical gradient of the mean wind speed in Case 2 agreed well with that in the observation, whereas the vertical gradient of the mean wind speed in Case 1 was smaller than that in the observation. At Location C, the observation data indicated that the vertical gradient of the mean wind speed at altitudes lower than 250 m was larger than that at altitudes higher than 250 m. This may be because of the inner boundary layer that developed rapidly when the wind flowed from the coastal area (smooth surface) to the urban area (rough surface) [12]. At Location C, the vertical gradient of the mean wind speed at altitudes lower than 250 m in Cases 1 and 2 was smaller than that in the observation, whereas the vertical gradient of the mean wind speed at altitudes higher than 250 m in Cases 1 and 2 agreed well with that in the observation.

By setting the roughness length based on the urban geometry, the accuracy in predicting the mean wind speed was improved significantly. However, it may be difficult for WRF-LES to simulate the rapid development of the inner boundary layer.

a) 10-min mean wind speed

b) 10-min mean wind direction
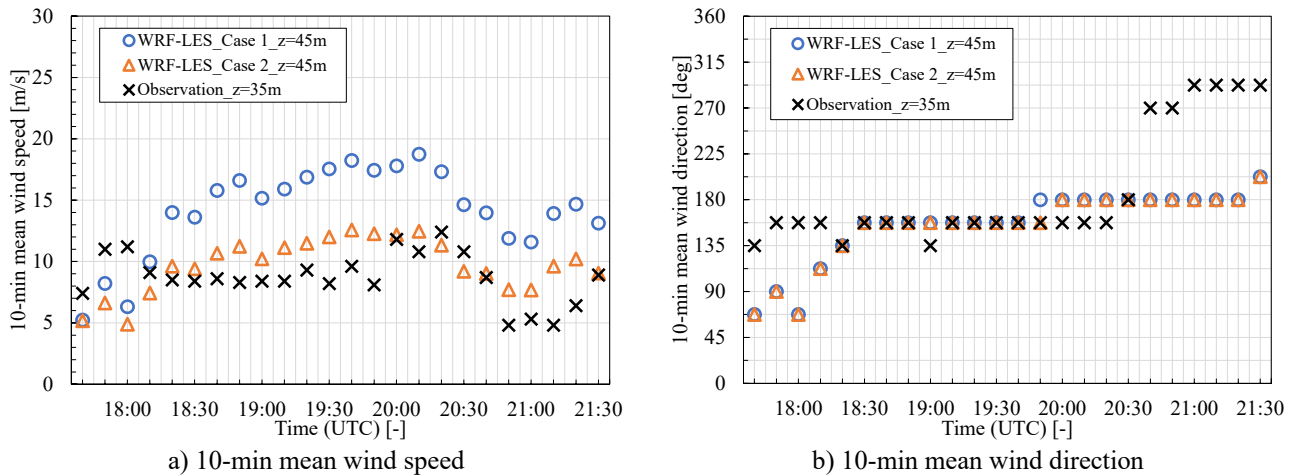
Figure 4: Time variation of 10-min mean wind speed and wind direction at Location A

a) Location A

b) Location B
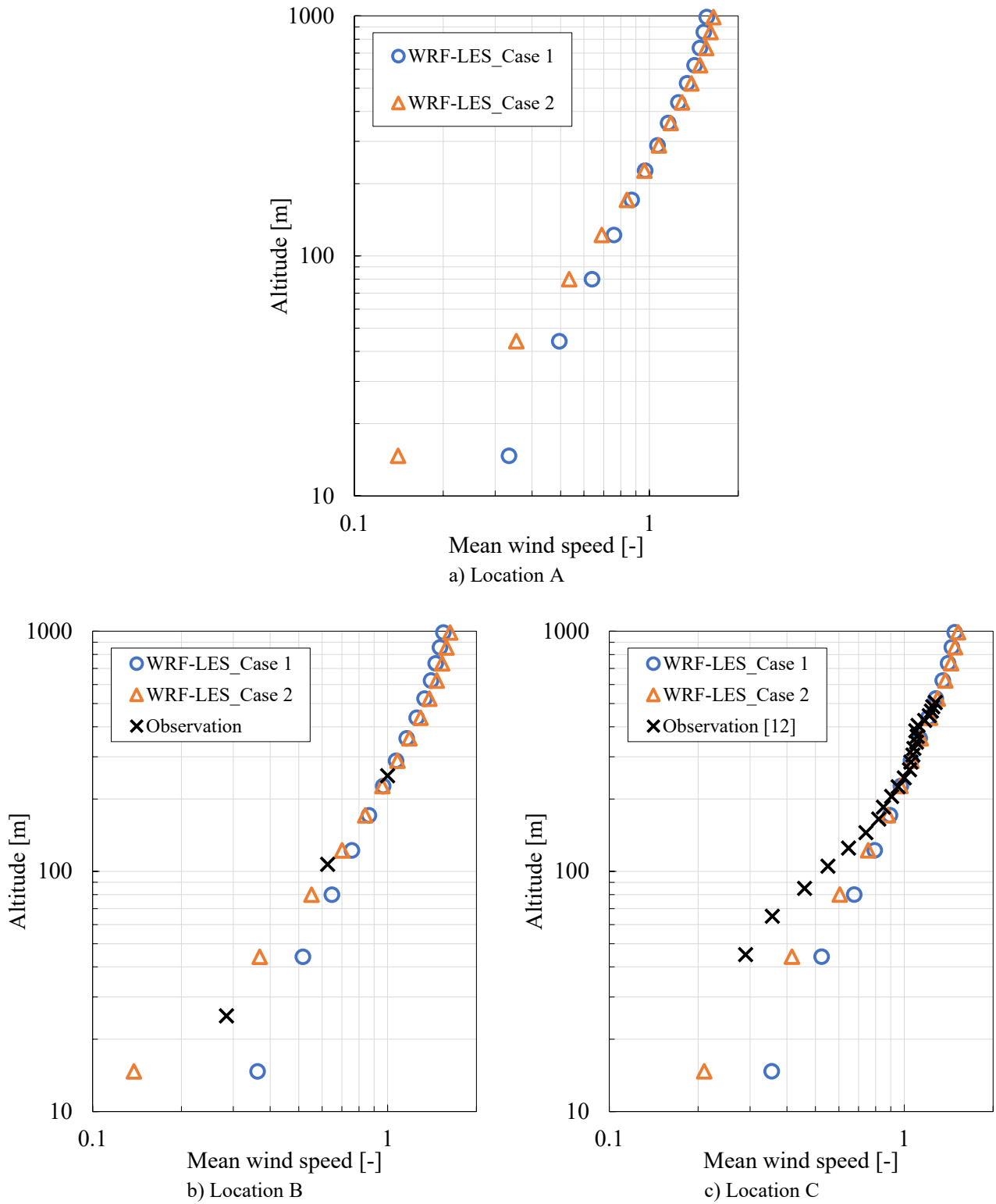
c) Location C

Figure 5: Vertical profile of mean wind speed at Location A, B and C (18:30 – 19:00)

3.3 Wind speed fluctuation (WRF-LES)

Figure 6 shows the time series data of the horizontal wind speed from 17:30 to 21:30 at Location A at an altitude of 45 m. In Case 2, the wind speed was lower than that in Case 1, but significant differences between Cases 1 and 2 were not seen in the characteristics of the wind speed fluctuation. The low-frequency wind speed fluctuation, which corresponds to several minute scale, occurred from 18:00 to 19:00 in both Cases 1 and 2. However, the high-frequency wind speed fluctuation, which was seen in the observation data, was not reproduced in the WRF-LES simulation. Figure 7 shows the spatial distribution of the horizontal wind speed at 18:30 at an altitude of 45 m. Although several kilometer scale flow structures, which are assumed to have been induced by the meteorological disturbance, were simulated, the high-frequency wind speed fluctuation was not seen in both Cases 1 and 2.

Figure 8 shows the vertical profile of the turbulence intensity from 18:30 to 19:00 at Location A. The turbulence intensity was defined as the ratio of the standard deviation of the wind speed fluctuation to the mean wind speed. In Figure 8, the vertical profile of the turbulence intensity for terrain category IV, which corresponds to middle-rise urban areas, in AIJ (Architectural Institute of Japan) wind load guideline [13] is also shown for reference. The difference between the results of Cases 1 and 2 was small, and WRF-LES underestimated the turbulence intensity, especially near the ground surface. This underestimation likely occurred because WRF-LES could not simulate the high-frequency wind speed fluctuation near the ground surface caused by the ground surface friction and the wake of buildings. However, at higher altitudes, where the contribution of the high-frequency wind speed fluctuation is assumed to be relatively small, the turbulence intensity in WRF-LES approached that in AIJ wind load guideline.

4 CONCLUSIONS

In this study, we investigated the influence of ground surface boundary conditions of WRF-LES on the accuracy in predicting the mean wind speed and wind speed fluctuation in the urban area. Two types of ground surface boundary conditions (Cases 1 and 2) were created. In Case 1, the roughness length for the urban area was set to 0.5 m uniformly (default setting), whereas in Case 2, the spatial distribution of roughness length for the urban area was set based on the urban geometry [6, 7, 8]. We performed the wind flow simulations in the central part of Tokyo during Typhoon Lan (2017) using WRF-LES with the created ground surface boundary conditions. The simulation results were compared with the observation data at multiple locations.

By setting the roughness length based on the urban geometry, the accuracy in predicting the mean wind speed in the urban area was improved significantly. However, in both cases, WRF-LES underestimated the turbulence intensity, especially near the ground surface. This underestimation likely occurred because WRF-LES could not simulate the high-frequency wind speed fluctuation near the ground surface caused by the ground surface friction and the wake of buildings. Therefore, it is necessary to add the high-frequency wind speed fluctuation using methods such as Kawai and Tamura [4] to generate LES inflow data from the simulation results of WRF-LES.
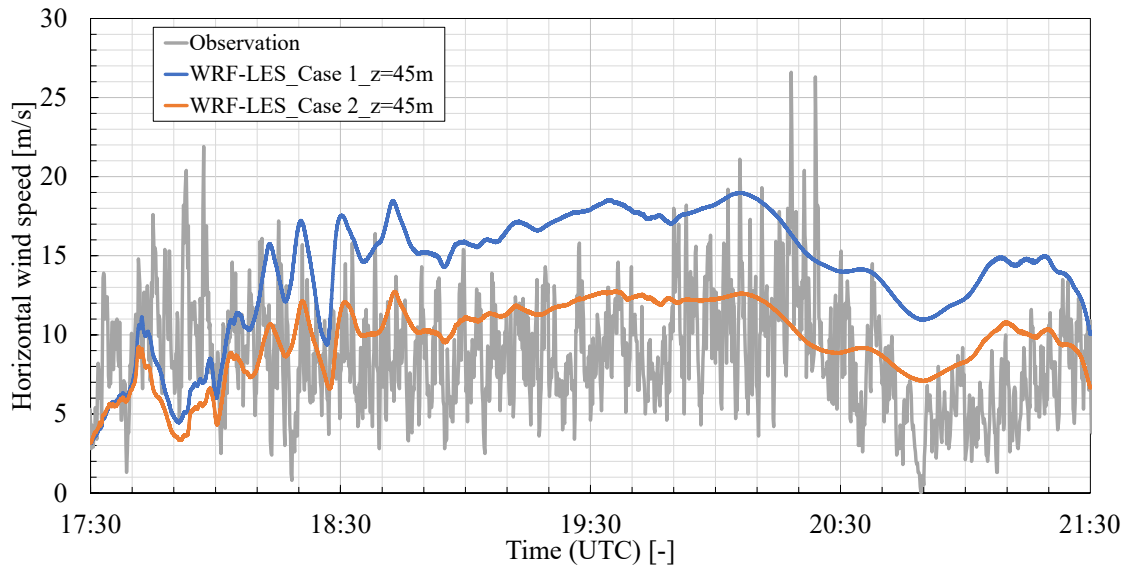
Figure 6: Time series data of horizontal wind speed at Location A at an altitude of 45 m (17:30 – 21:30)

a) Case 1   b) Case 2
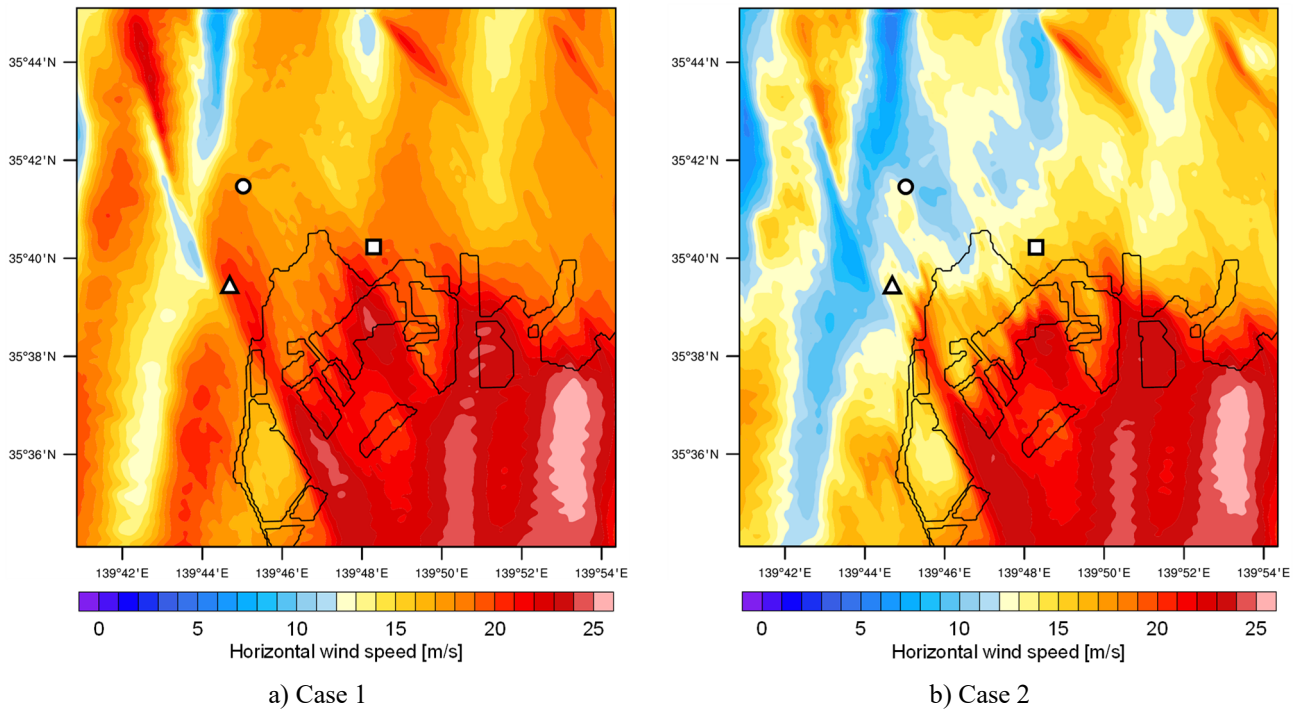
Figure 7: Spatial distribution of horizontal wind speed at an altitude of 45 m in Domain 5 (18:30)
(○: Location A (Tokyo District Meteorological Observatory), △: Location B (Tokyo Tower) and □: Location C (Kiba))
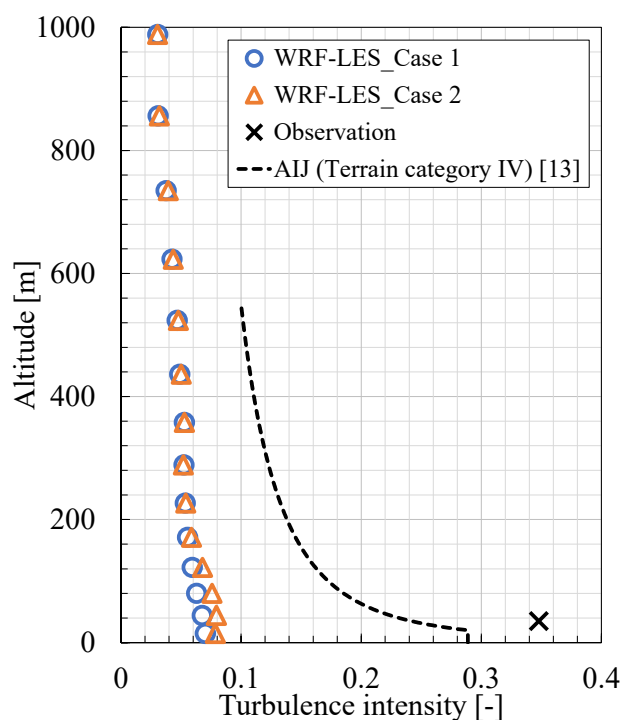
Figure 8: Vertical profile of turbulence intensity at Location A (18:30 – 19:00)

REFERENCES

[1] Etling, D. and Brown, R.A. Roll vortices in the planetary boundary layer: A review. *Boundary-Layer Meteorology* (1993) **65**: 215-248.

[2] Weckwerth, T.M., Horst, T.W. and Wilson, J.W. An Observational Study of the Evolution of Horizontal Convective Rolls. *Monthly Weather Review* (1999) **127**: 2160-2179.

[3] Nakanishi, M. and Niino, H. Large-Eddy Simulation of Roll Vortices in a Hurricane Boundary Layer. *Journal of the Atmospheric Science* (2012) **69**: 3558-3575.

[4] Kawai, H. and Tamura, T. Method for adding high frequency components to a velocity field obtained from a mesoscale meteorological model: Application of spatial filtering and rescaling method. *Journal of Structural and Construction Engineering (Transactions of Architectural Institute of Japan)* (2020) **85**: 19-27. (in Japanese)

[5] Nakajima, K., Kawai, H., Kawaguchi, M., Tamura, T., Kondo, K., Itoh, Y. and Takagi, K. Numerical simulation of wind flow during typhoon No. 21 (2017) in central part of Tokyo using WRF-LES. *Summaries of Technical Papers of Annual Meeting, Architectural Institute of Japan* (2021). (in Japanese)

[6] Kanda, M., Inagaki, A., Miyamoto, T., Gryschka, M. and Raasch, S. A New Aerodynamic Parametrization for Real Urban Surfaces. *Boundary-Layer Meteorology* (2013) **148**: 357-377.

[7] Makabe, T., Nakayoshi, M., Varquez, A.C.G. and Kanda, M. Database of meteorological urban geometric parameters of Japan and extension to global scale. *Journal of Japan Society of Civil Engineers* (2014) **70**: 331-336. (in Japanese)

[8] Kanda, M. *Data Integration and Analysis System* (2014).

[9] Skamarock, W.C., Klemp, J.B., Dudhia, J., Gill, D.O., Barker, D.M., Duda, M.G., Huang, X.Y., Wang, W. and Powers, J.G. A Description of the Advanced Research WRF Version 3. *NCAR Technical Note* (2008).

[10] Hong, S.Y., Noh, Y. and Dudhia, J. A New Vertical Diffusion Package with an Explicit Treatment of Entrainment Processes. *Monthly Weather Review* (2006) **134**: 2318-2341.

[11] Lilly, D.K. The representation of small-scale turbulence in numerical simulation experiments. *IBM Scientific Computing Symposium on Environmental Sciences* (1967).

[12] Yamanaka, T., Nakajima, K., Ooka, R., Kikumoto, H. and Sugawara, H. Wind observation for evaluation of design wind speed at high altitude using Doppler lidar (Part 2) Strong wind case by Typhoon No.21 in 2017. *Summaries of Technical Papers of Annual Meeting, Architectural Institute of Japan* (2018). (in Japanese)

[13] Architectural Institute of Japan. Recommendations for Loads on Buildings. *Architectural Institute of Japan* (2015).